LETTERS

Planar cell polarity signalling couples cell division and morphogenesis during neurulation

Brian Ciruna[1]†, Andreas Jenny[2], Diana Lee[1], Marek Mlodzik[2] & Alexander F. Schier[1]†

Environmental and genetic aberrations lead to neural tube closure defects (NTDs) in 1 out of every 1,000 births[1]. Mouse and frog models for these birth defects have indicated that Van Gogh-like 2 (Vangl2, also known as Strabismus) and other components of planar cell polarity (PCP) signalling might control neurulation by promoting the convergence of neural progenitors to the midline[2–8]. Here we show a novel role for PCP signalling during neurulation in zebrafish. We demonstrate that non-canonical Wnt/PCP signalling polarizes neural progenitors along the anteroposterior axis. This polarity is transiently lost during cell division in the neural keel but is re-established as daughter cells reintegrate into the neuroepithelium. Loss of zebrafish Vangl2 (in *trilobite* mutants) abolishes the polarization of neural keel cells, disrupts re-intercalation of daughter cells into the neuroepithelium, and results in ectopic neural progenitor accumulations and NTDs. Remarkably, blocking cell division leads to rescue of *trilobite* neural tube morphogenesis despite persistent defects in convergence and extension. These results reveal a function for PCP signalling in coupling cell division and morphogenesis at neurulation and indicate a previously unrecognized mechanism that might underlie NTDs.

During zebrafish neurulation the neural plate folds towards the midline. This results in the apposition of apical surfaces from opposite sides of the neural plate and the formation of the neural keel (Supplementary Fig. 1). As cells divide, one daughter cell remains in the ipsilateral side of the neural keel, whereas the other daughter cell intercalates across the midline and integrates into the contralateral neuroepithelial layer[9–11]. To explore the molecular basis of neural progenitor cell morphogenesis we used a candidate gene approach and examined whether the PCP signalling component Vangl2 might be involved[12,13]. We eliminated all Vangl2 activity by generating maternal-zygotic *trilobite* (MZ*tri*) mutants with the use of a germline-replacement strategy[14]. MZ*tri* embryos proved more severely affected than zygotic mutants (Supplementary Fig. 2). Comparison of wild-type (WT) and mutant embryos at the 20-somite stage revealed that MZ*tri* embryos do not generate a normal neural tube (Fig. 1g, h). The MZ*tri* neural anlage develops as an outer pseudo-stratified neuroepithelial layer surrounding an ectopic mass of disorganized cells (Fig. 1h). As early as the neural keel stage, the MZ*tri* neural primordium appears broader and thicker than in WT (Fig. 1c, d). This trend continues through neural rod stages when cells seem to accumulate in the centre of the wide MZ*tri* neural anlage (Fig. 1e, f). The floorplate of MZ*tri* mutant embryos also appears broader than in WT (Fig. 1e–h), as is evident in sections through *sonic hedgehog*-stained WT and MZ*tri* embryos (Supplementary Fig. 8e, g). Expanded neural midline structures are also characteristic of frog and mouse PCP signalling mutants[2,8].

Because Vangl2 has been shown to modulate the non-canonical Wnt signalling pathway, we asked whether Wnt signals also regulate neural tube morphogenesis. Using a modified germline-replacement protocol (Supplementary Fig. 3), we generated *wnt11/silberblick (slb)*[15] and *wnt5/pipetail (ppt)*[16] MZ compound mutants (Supplementary Fig. 4). MZ*slb;*MZ*ppt* embryos showed a similar, yet less severe, neurulation phenotype to that of MZ*tri* mutants (Fig. 1i). Reduction of Wnt4 activity in an MZ*slb;*MZ*ppt* background (through injection of *wnt4* antisense morpholino oligonucleotides[17]) enhanced the mutant phenotype, and at the 20-somite stage MZ*slb;*MZ*ppt;wnt4*-morphant embryos displayed a neurulation phenotype very similar to that of MZ*tri* mutants (Fig. 1j, and Supplementary Fig. 4). These results indicate that non-canonical Wnt signalling is required for normal zebrafish neurulation.

In the frog, neural tube closure requires PCP signalling within the neural plate[18]. To determine whether MZ*tri* neurulation defects are autonomous to the neuroectoderm or secondary to mesoderm or endoderm convergence and extension defects, we examined neurulation in embryos lacking endoderm and trunk and head mesoderm. Such embryos were generated by misexpression of Lefty, an inhibitor of Nodal signalling[19,20]. MZ*tri* + *lefty* embryos were considerably shorter than WT + *lefty* controls (compare Fig. 2a with Fig. 2b), and had neurulation defects similar to MZ*tri* mutants (Fig. 2b, inset). In a complementary assay, we examined whether mutant mesendoderm can induce the MZ*tri* neurulation phenotype. We generated chimaeric embryos in which only the endoderm and trunk mesoderm lineages were derived from MZ*tri* mutant cells (Fig. 2c). In these embryos the neural tube developed with normal neuroepithelial morphology, a well-formed neurocoel and no evidence of ectopic cell accumulations (Fig. 2c′). These results indicate that MZ*tri* neurulation defects are due to the lack of Vangl2 function in ectodermal tissues.

Several potential mechanisms might underlie the ectopic accumulation of cells seen in MZ*tri* mutants, including abnormal delamination of neuroepithelial cells or failed reintegration of cells into the neuroepithelium after cell division. As a first test to distinguish between these possibilities, we used the photoconvertible Kaede fluorophore[21] to label half of the neuroepithelium at neural plate or early neural keel stages and then analysed the location of the labelled cells and their descendants in the neural tube (Fig. 3a–d). In agreement with previous studies of zebrafish neurulation[9–11], we observed that cell division in the neural keel results in the bilateral distribution of daughter cells across apposing neuroepithelial layers of the WT neural tube ($n = 10$; Fig. 3a, b). In marked contrast, labelled cells were not found in the contralateral neuroepithelium of MZ*tri* embryos ($n = 29$), and a sharp midline boundary was maintained even among cells accumulating ectopically in the neural anlage

[1]Developmental Genetics Program, Skirball Institute of Biomolecular Medicine and Department of Cell Biology, New York University School of Medicine, New York, New York 10016, USA. [2]Mount Sinai School of Medicine, Brookdale Department of Molecular, Cellular and Developmental Biology, 1 Gustave L. Levy Place, New York, New York 10029, USA. †Present addresses: Program in Developmental Biology, The Hospital for Sick Children, Toronto Medical Discovery Tower, Toronto, Ontario M5G 1L7, Canada (B.C.); Department of Molecular and Cellular Biology, Harvard University, Cambridge, Massachusetts 02138, USA (A.F.S.).

(Fig. 3c, d). These results are consistent with a defect in the integration of MZ*tri* neural progenitors into the contralateral neuroepithelium.

To follow more directly the behaviour of neural progenitors during and after mitosis, we imaged cell behaviour in the neural keel of WT ($n = 14$) and MZ*tri* mutant ($n = 11$) embryos (Fig. 3e–m). As observed previously, we found that WT cells rounded up and divided apically—that is, along the medial–lateral axis of the neural keel—and that daughter cells became incorporated into opposite sides of the neural tube (Fig. 3e–g, and Supplementary movie 1)[10,11]. In addition, we found that the more basal daughter cell maintained contact with the basement membrane through a thin cellular process (Fig. 3e, f, arrow) and returned to its original position within the neuroepithelium. In contrast, the more apical daughter cell lost contact with the basement membrane, became polarized across the medial–lateral axis and intercalated across the midline into the contralateral side of the neural keel (Fig. 3f, g, arrowhead). Intercalation of apical daughter cells across the midline took an average of 8 min after completion of cytokinesis (data not shown).

In MZ*tri* embryos, cell division seemed normal. Cells divided apically, and basal daughter cells maintained their ipsilateral position within the neuroepithelium (Fig. 3h, i, arrow). In notable contrast to the wild type, however, apical MZ*tri* daughter cells failed to reintegrate into the neuroepithelium after mitosis (Fig. 3i, j, arrowhead). These daughter cells accumulated in the middle of the MZ*tri* neural anlage and remained in the place where they were formed (Fig. 3j, and Supplementary Fig. 5). To determine whether MZ*tri* intercalation defects were secondary to abnormal neural tube morphogenesis, we examined cell division at the onset of neural keel formation, before an obvious MZ*tri* neurulation phenotype (compare Fig. 1a, b). We observed that after mitosis, apical MZ*tri* daughter cells failed to intercalate across the midline (Fig. 3k–m, and Supplementary movie 2). These results indicate that the PCP pathway is required for the intercalation of neural progenitor cells into the contralateral neuroepithelial layer after cell division in the neural keel.

PCP signalling functions to polarize cells, but molecular evidence for such a role during neurulation has been elusive. We therefore analysed the subcellular localization of PCP signalling components[22,23] and examined whether the failure of MZ*tri* cell re-intercalation is due to polarity defects. We found that enhanced green fluorescent protein (EGFP)-tagged Prickle[24] (Gfp-Pk), a PCP effector molecule, showed striking asymmetric localization in WT cells of the notochord and neural keel (Fig. 4a, d). This fusion protein was functional and rescued zebrafish Pk1-morphants

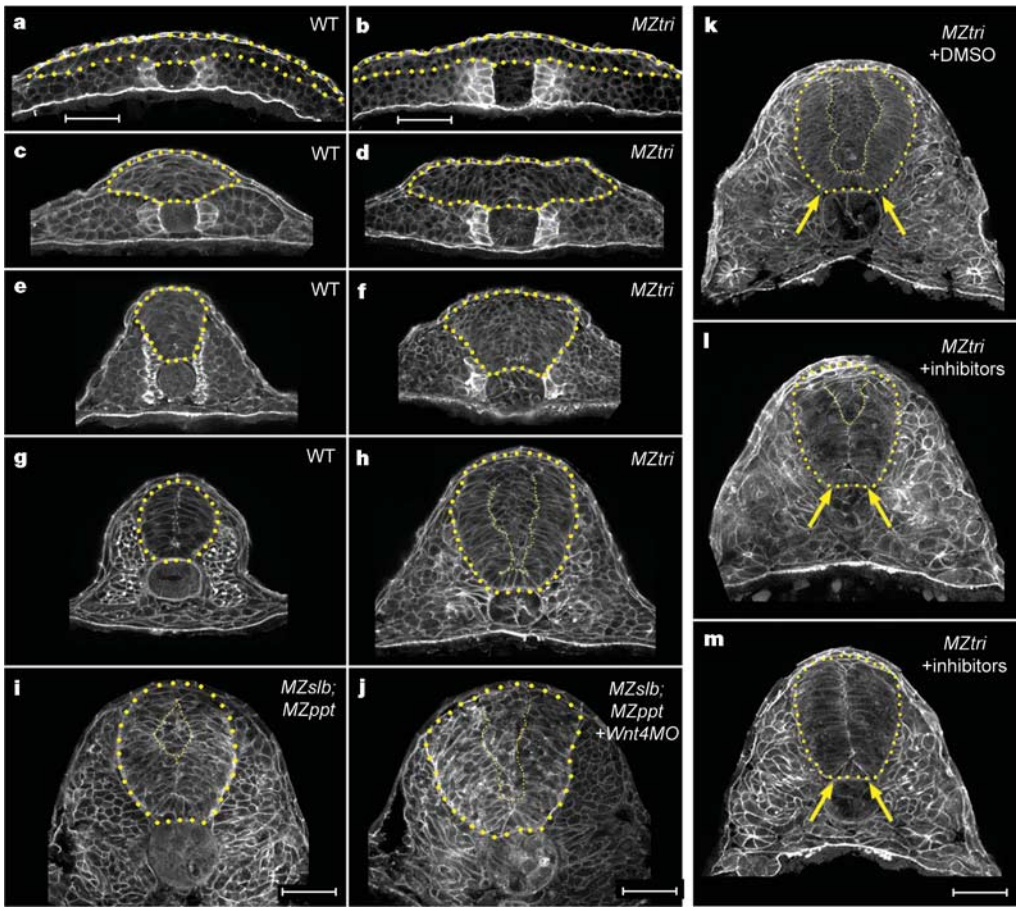

Figure 1 | PCP signalling is required for zebrafish neural tube formation. **a**–**h**, Confocal micrographs of transverse sections through rhodamine-phalloidin-stained embryos, comparing WT and MZ*tri* neural tube morphogenesis at five-somite/neural plate (**a**, **b**), ten-somite/neural keel (**c**, **d**), 15-somite/neural rod (**e**, **f**) and 20-somite/neural tube (**g**, **h**) stages. The neural anlage is outlined in all images. **i**, **j**, Sections through mGFP-injected 20-somite-stage embryos showing ectopic cell accumulations within the developing neural tube of MZ*slb;*MZ*ppt* embryos (**i**), and severe disorganization of the neural anlage in MZ*slb;*MZ*ppt* embryos that had been injected with 6 ng of Wnt4 morpholino antisense oligonucleotides (**j**). **k**–**m**, Rhodamine-phalloidin-stained sections through 20-somite-stage MZ*tri* embryos cultured overnight either in 4% dimethylsulphoxide (**k**) or in the presence of the DNA synthesis inhibitors aphidicolin and hydroxyurea[25] (**l**, **m**). Note the rescue of the expanded floorplate (arrows in **k**–**m**) and defects in neural tube morphogenesis on blocking of cell division. The extent of ectopic cellular accumulations in PCP signalling mutants is outlined (**h**–**l**). Scale bars, 50 μm.

(Supplementary Fig. 6). Gfp-Pk was present predominantly in the cytoplasm but became asymmetrically localized to distinct, dynamic puncta along the anterior membrane of neural keel cells (Fig. 4a, arrows, and Supplementary movie 3). Membrane localization of Gfp-Pk was lost during cell division in the neural keel (Fig. 4e) but was subsequently re-established in both daughter cells (Fig. 4f). To determine whether this localization is dependent on PCP signalling, we analysed MZ*tri* and MZ*slb;*MZ*ppt;wnt4*-morphant embryos (Fig. 4b, c). In both contexts the asymmetric localization of Gfp-Pk was severely reduced or absent. These results establish membrane localization of Gfp-Pk as the first molecular marker of planar polarity in neural progenitors and reveal that PCP signalling polarizes cells across the anteroposterior (AP) axis.

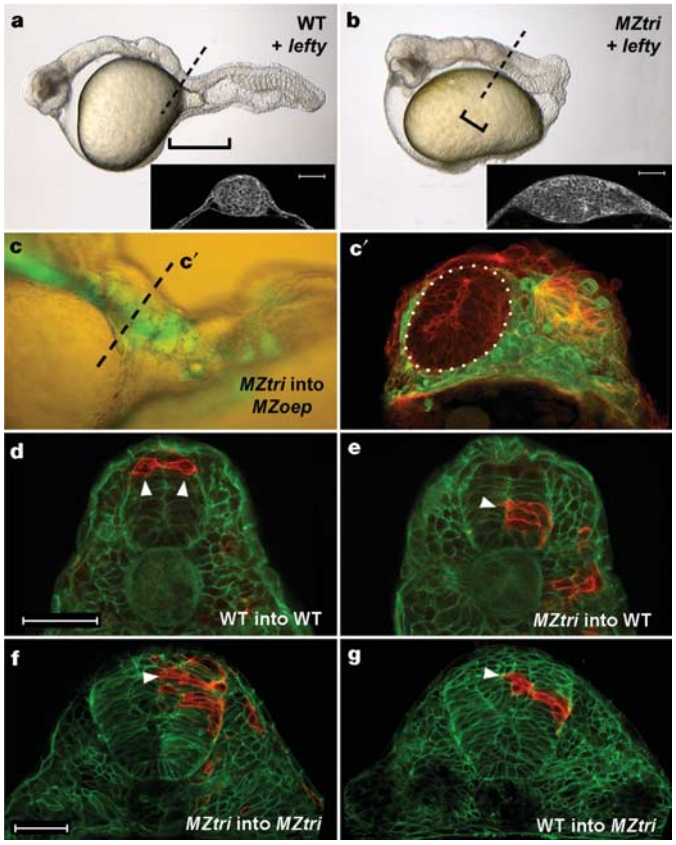

Figure 2 | Cell autonomy of PCP signalling within the neural keel. **a**, **b**, Whole mounts and transverse sections through the trunk of WT (**a**) and MZ*tri* (**b**) embryos 24 h after fertilization, injected with 100 pg of *lefty* mRNA. Convergence of the neural plate into a neural rod occurs normally in WT + *lefty* embryos (**a**), despite the absence of underlying mesendoderm (inset, section indicated by dotted line. This convergence is disrupted in MZ*tri* + *lefty* mutants (**b**), which show neurulation defects in the absence of trunk mesoderm (inset, section indicated by dotted line). Brackets in **a** and **b** indicate the extent of trunk axial extension. Identical results were obtained with a different genetic combination: maternal-zygotic *one-eyed-pinhead* (MZ*oep*) mutants were used to eliminate Nodal signalling, and PCP signalling was perturbed through the injection of *diego* mRNA (not shown). **c**, mGFP-labelled MZ*tri* cells were transplanted into MZ*oep* host embryos at mid-blastula stages to generate MZ*tri* → MZ*oep* chimaeric embryos. MZ*oep* mutants lack Nodal signalling and do not form endoderm or trunk mesoderm lineages[29]; endoderm and trunk somites in chimaeric embryos therefore develop entirely from GFP-positive MZ*tri* donor cells. **c′**, Transverse sections of MZ*tri* → MZ*oep* chimaeras 24 h after fertilization were counterstained with rhodamine-phalloidin to visualize neural tube formation (outlined with a dotted line). The absence of MZ*tri* neurulation defects indicates a requirement for PCP signalling autonomous to the neuroectoderm. **d**–**g**, Transverse sections through the trunk of WT and MZ*tri* chimaeric embryos at 24 h after fertilization. **d**, Bilateral distribution of mRFP-labelled WT cells (arrowheads) within the neural tube of an mGFP-labelled WT host. **e**, Unilateral accumulation of mRFP-labelled MZ*tri* cells within the neural tube of mGFP-labelled WT host embryos. **f**, **g**, mRFP-labelled MZ*tri* (**f**) or WT (**g**) cells transplanted into mGFP-labelled MZ*tri* host embryos accumulate unilaterally within the MZ*tri* neural anlage. Scale bars, 50 μm.

To determine the cell autonomy of Vangl2 function and Gfp-Pk localization during neurulation, we generated chimaeras of WT and MZ*tri* cells (Supplementary Table 1). When WT donor cells were transplanted into WT hosts, most donor clones distributed daughter cells into the contralateral side of the neural tube (88% of clones, $n = 16$; Fig. 2d). In contrast, only a minority of MZ*tri* donor clones in the neural tube of WT hosts (38%, $n = 37$) showed contralateral cell intercalation, despite the normal morphogenesis of the surrounding WT neuroepithelial tissue (Fig. 2e). Time-lapse analysis of MZ*tri* cell behaviour in WT neural keels showed that most MZ*tri* daughter cells ($n = 4$ of 6) failed to intercalate across the midline after mitosis, indicating a cell-autonomous role for Vangl2 (Supplementary Fig. 7a–c). MZ*tri* cells transplanted into WT host embryos also failed to localize Gfp-Pk to the membrane (Fig. 4g). In cases where MZ*tri* cells showed some evidence of medial–lateral intercalation, the rate of cell movement was severely delayed ($n = 2$ of 6; Supplementary Fig. 7d–f).

Most MZ*tri* donor clones in MZ*tri* hosts showed no evidence of cell intercalation across the midline (95%, $n = 41$; Fig. 2f). Similarly, in transplantations of WT cells into MZ*tri* hosts, 93% of donor clones did not intercalate into the contralateral neuroepithelium ($n = 61$; Fig. 2g). Time-lapse analysis of WT cell behaviour in a MZ*tri* neural keel confirmed that WT neural progenitors fail to polarize and re-intercalate after mitosis ($n = 7$; Supplementary Fig. 7g–i). Strikingly, WT cells transplanted into MZ*tri* hosts also showed a decrease in membrane-localized Gfp-PK and a loss in AP polarity (Fig. 4h), indicating that non-autonomous effects on neurulation are not simply the result of a passive obstruction to cell intercalation. These results indicate that Vangl2 might be required both autonomously in cells that must reintegrate into the neuroepithelium and non-autonomously in neighbouring cells in order to establish or maintain planar polarity in neural progenitors.

Our results show that PCP signalling is required for the repolarization and reintegration of neural progenitors after cell division in the neural keel. Indeed, the predominant role of PCP signalling might be to counteract the morphogenetic consequences of mitosis, which results in loss of polarity and the exclusion of apical daughter cells from the neuroepithelium. The strictest inference of this model would be that MZ*tri* neurulation defects may be suppressed by blocking cell division, thus precluding the need for PCP signalling. We therefore attempted to block cell division in WT and MZ*tri* embryos through application of the DNA synthesis inhibitors aphidicolin and hydroxyurea[25]. Mitotic inhibitors were applied at late gastrulation stages to target maximal effects on neurulation. Treatment with inhibitor significantly decreased the incidence of contralateral cell intercalation of WT neural progenitors (Supplementary Table 1), but neurulation proceeded normally in treated WT embryos (Supplementary Fig. 8). Strikingly, blocking cell division suppressed MZ*tri* neurulation defects in 90% of embryos ($n = 41$; Fig. 1 k–m, and Supplementary Fig. 8) and rescued neural tube morphogenesis, aberrant floorplate expansion and ectopic neural progenitor accumulations in 62% of these cases (Fig. 1m). This result indicates that PCP signalling is no longer required for neural tube formation if cell division is blocked.

Taken together, our studies indicate that through re-establishing cell polarity and directing intercalative behaviour, PCP signalling might function to correct for the morphogenetic consequences of mitoses on neural tube morphogenesis. First, in the neural plate, midline progenitors distribute daughter cells along the medial–lateral axis, thus broadening the neural midline and future floor-

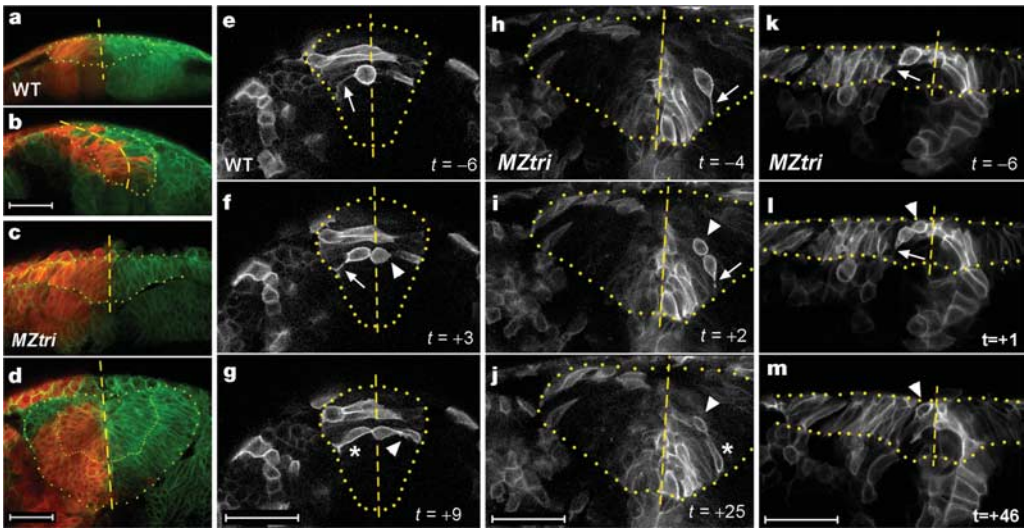

Figure 3 | The cellular basis of MZ*tri* neurulation defects. **a**–**d**, Lineage tracing of WT (**a**, **b**) and MZ*tri* (**c**, **d**) neural plate cells after red photoconversion of the Kaede fluorophore. WT neural progenitors routinely crossed the midline into the contralateral side of the neural tube (**b**). MZ*tri* neural progenitor cells never integrated into the contralateral neuroepithelium (**d**). Cells accumulating ectopically in the centre of the MZ*tri* neural anlage also respected the midline (dashed lines). **e**–**m**, Confocal micrographs from time series depicting cell division during WT (**e**–**g**) and MZ*tri* (**h**–**m**) neurulation. Time *t* is indicated as minutes before or after the completion of cytokinesis. The boundary of the neural keel has been highlighted, and the midline indicated. Cells in the WT neural keel round up their cell bodies and divide apically (**e**). Basal daughter cells remain connected to the basement membrane through a cellular process (arrow in **e** and **f**) and reinsert into the neuroepithelium (asterisk in **g**). Apical daughter cells (arrowhead in **f** and **g**) lose contact within the basal membrane, adopt medial–lateral polarity and intercalate across the midline of the neural keel. MZ*tri* cells divide apically, and basal daughter cells behave as in WT (arrow in **h**, **i**, **k** and **l**; asterisk in **j**). MZ*tri* apical daughter cells (arrowhead in **i**, **j**, **l** and **m**) do not intercalate into the contralateral neuroepithelium and remain in the place where they were formed. Scale bars, 50 μm.

plate[11]. PCP-mediated convergence of midline cells counters this broadening[2–8]. Second, neural keel cells divide apically and position daughter cells outside the neuroepithelium. PCP-mediated reintegration of neural progenitors ensures that these cells do not accumulate in the midline. Although our results do not exclude additional roles for PCP signalling during neural development, blocking cell division abrogates the need for PCP signalling during neurulation and suppresses the floorplate and neural tube phenotypes associated with MZ*tri* mutants.

Our results contrast with a recent study[26] that analysed the role of PCP signalling during earlier stages of zebrafish development. It was shown that PCP signalling functions upstream of mitosis to orient the plane of cell division at gastrulation. At this stage, PCP signals instruct neural precursors to divide along the animal–vegetal axis, thus driving extension of the zebrafish axis. Conversely, our study indicates that PCP signalling functions after mitosis to counteract the morphogenetic consequences of cell divisions during neurulation. Although the molecular basis of this process is unknown, it is possible that PCP signalling regulates molecules involved in the establishment of apical–basal polarity or cell adhesion, two processes that might be disrupted by mitosis[27]. It also remains to be determined whether components of the mitotic apparatus directly regulate the re-establishment of planar polarity. No matter what the precise molecular underpinnings might be, our study shows that PCP signalling is required to compensate for the morphogenetic consequences of cell division on neural tube morphogenesis by promoting the polarity and intercalation of neural progenitors. Neural tube closure defects in *curly tail* (*ct*) mice, a genetic model for human NTDs, can also be modulated with agents that slow the rate of embryonic cell division[28]. Pharmacological inhibition of cell division at gastrula stages exacerbates the *Ct* NTD phenotype, whereas treatment during neurulation rescues closure defects of the neural tube[28]. Although the nature of the *Ct* mutation and the mechanism of pharmacological rescue remain unclear, our results raise the possibility that the uncoupling of PCP signalling and cell division during neurulation represent a common origin of neural tube closure defects.

METHODS

Strains. The following mutants were used: *ppt(sk13)* (Supplementary Fig. 4), *slb(tx226)*[15], *tri(tk50f)*[13] and MZ*oep(tz57)*[29]. Germline-replacement chimaeras for *tri* were generated as described previously[14]. The generation of germline-replacement chimaeras for *slb;ppt* compound mutants is described in Supplementary Fig. 3.

Embryo microinjection and transplantation. Plasmids containing membrane-localized GFP (*mGFP*), membrane-localized red fluorescent protein RFP (*mRFP*), EGFP-tagged Prickle (*Gfp-Pk*)[24], *Kaede*[21] or *lefty*[19,20] were linearized and sense-strand-capped mRNA was synthesized with the mMESSAGE mMACHINE system (Ambion). Morpholino antisense oligonucleotides (Gene Tools) were designed for zebrafish *Pk1* (ref. 30) and *Wnt4* (ref. 17) as described previously. Zebrafish embryos were dechorionated by treatment with pronase and injected at the one-cell stage. Scatter labelling was obtained by injecting a subset of blastomeres at the 16-cell to 32-cell stage. Cell transplantations were performed at mid-blastula stages, as described previously[14]. For chimaeric analyses of Vangl2 function, one-cell-stage WT and MZ*tri* embryos were injected with 100 pg of either *mRFP* or *mGFP* mRNA. At mid-blastula stages, about 30–50 donor cells were transplanted into a single location above the margin of host embryos, to ensure unilateral distribution of donor cell clones within the anterior spinal cord of host embryos.

Cell division inhibitors. To block cell division at neurulation, embryos were cultured in a solution of 150 μM aphidicolin (Sigma) and 20 mM hydroxyurea (Sigma) in 4% dimethylsulphoxide[25], beginning at 80% epiboly stages.

Sectioning and microscopy. For transverse sections, embryos were fixed overnight in 4% paraformaldehyde, embedded in 2% agarose and sectioned on a vibratome into 200-μm slices. Live embryos were mounted in 0.8% agarose before imaging. Fluorescent images of embryos injected with mGFP, mRFP or Gfp-Pk, or samples stained with rhodamine-phalloidin (Molecular Probes) were obtained with a Zeiss LSM510 confocal microscope. For live imaging of cell divisions within the neural keel, embryos were scatter-labelled with mGFP and imaging was performed in a transverse plane through the trunk of 6–12-somite-stage embryos at the first to sixth somite level.

Lineage tracing. Embryos were injected with 100 pg of *Kaede* mRNA and 100 pg of *mGFP* mRNA (for contrast) at the one-cell stage, developed in the dark until

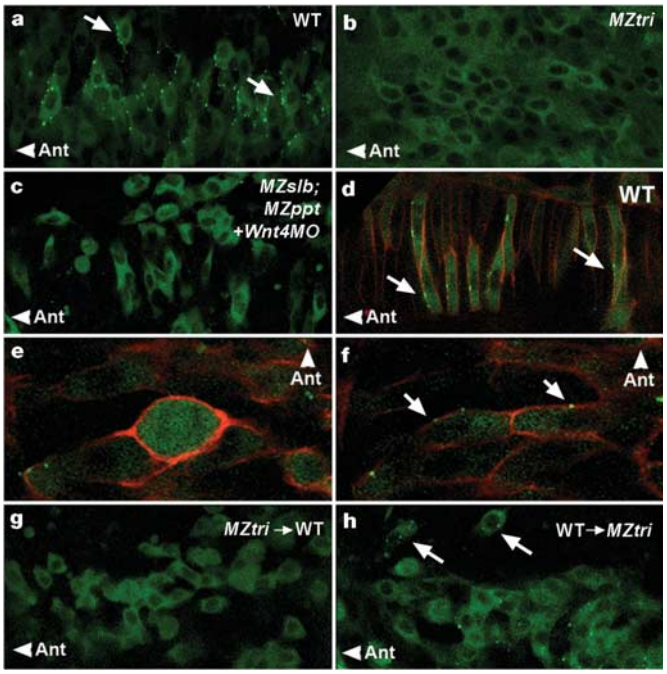

Figure 4 | Anterior membrane localization of Gfp-Pk as a marker of planar polarity. Confocal images taken at the level of the anterior spinal cord, through the dorsal–ventral plane of the neural keel (**a**–**c**, **e**–**h**) or notochord (**d**) of 8–10-somite-stage embryos. **a**–**c**, Scatter labelling of Gfp-Pk in the neural keel of a WT embryo (**a**), an MZ*tri* mutant (**b**) or an MZ*slb*;MZ*ppt* mutant (**c**) injected with 6 ng of *Wnt4* morpholino antisense oligonucleotides. **d**, Scatter labelling of Gfp-Pk plus mRFP in WT notochord, showing anterior membrane translocation of Gfp-Pk (arrows) in cells that undergo well-characterized convergence and extension movements in response to PCP signalling. **e**, **f**, A WT neural keel cell labelled with Gfp-Pk and mRFP, showing transient loss of polarity markers during mitosis (**e**) but re-establishment of membrane-localized Gfp-Pk in both daughter cells (**f**, arrows). **g**, **h**, Chimaeric analysis of the autonomy of PCP signalling, using Gfp-Pk as a marker of planar polarity. **g**, MZ*tri* cells transplanted into WT host embryos do not localize Gfp-Pk to the membrane, because Vangl2 is required for Pk translocation. **h**, WT cells transplanted into MZ*tri* hosts show reduced membrane Gfp-Pk localization and abnormal polarity (arrows). Ant, anterior direction.

five-to-six-somite stages, and live-mounted in 0.8% agarose. The Kaede fluorophore was converted from green to red by focusing a 60-s pulse of ultraviolet light specifically on one lateral half of the neural plate, using the pinhole of a Zeiss LSM510 confocal microscope. Embryos were imaged both immediately and 10 h after treatment with ultraviolet light.

Received 6 September; accepted 26 October 2005.

1. Copp, A. J., Greene, N. D. & Murdoch, J. N. The genetic basis of mammalian neurulation. *Nature Rev. Genet.* **4,** 784–793 (2003).
2. Greene, N. D., Gerrelli, D., Van Straaten, H. W. & Copp, A. J. Abnormalities of floor plate, notochord and somite differentiation in the loop-tail (Lp) mouse: a model of severe neural tube defects. *Mech. Dev.* **73,** 59–72 (1998).
3. Kibar, Z. *et al.* Ltap, a mammalian homolog of *Drosophila* Strabismus/Van Gogh, is altered in the mouse neural tube mutant Loop-tail. *Nature Genet.* **28,** 251–255 (2001).
4. Murdoch, J. N., Doudney, K., Paternotte, C., Copp, A. J. & Stanier, P. Severe neural tube defects in the loop-tail mouse result from mutation of Lpp1, a novel gene involved in floor plate specification. *Hum. Mol. Genet.* **10,** 2593–2601 (2001).
5. Keller, R. Shaping the vertebrate body plan by polarized embryonic cell movements. *Science* **298,** 1950–1954 (2002).
6. Wallingford, J. B., Fraser, S. E. & Harland, R. M. Convergent extension: the molecular control of polarized cell movement during embryonic development. *Dev. Cell* **2,** 695–706 (2002).
7. Goto, T. & Keller, R. The planar cell polarity gene strabismus regulates convergence and extension and neural fold closure in *Xenopus*. *Dev. Biol.* **247,** 165–181 (2002).
8. Wallingford, J. B. & Harland, R. M. Neural tube closure requires Dishevelled-dependent convergent extension of the midline. *Development* **129,** 5815–5825 (2002).
9. Kimmel, C. B., Warga, R. M. & Kane, D. A. Cell cycles and clonal strings during formation of the zebrafish central nervous system. *Development* **120,** 265–276 (1994).
10. Concha, M. L. & Adams, R. J. Oriented cell divisions and cellular morphogenesis in the zebrafish gastrula and neurula: a time-lapse analysis. *Development* **125,** 983–994 (1998).
11. Geldmacher-Voss, B., Reugels, A. M., Pauls, S. & Campos-Ortega, J. A. A 90-degree rotation of the mitotic spindle changes the orientation of mitoses of zebrafish neuroepithelial cells. *Development* **130,** 3767–3780 (2003).
12. Park, M. & Moon, R. T. The planar cell-polarity gene *stbm* regulates cell behaviour and cell fate in vertebrate embryos. *Nature Cell Biol.* **4,** 20–25 (2002).
13. Jessen, J. R. *et al.* Zebrafish trilobite identifies new roles for Strabismus in gastrulation and neuronal movements. *Nature Cell Biol.* **4,** 610–615 (2002).
14. Ciruna, B. *et al.* Production of maternal-zygotic mutant zebrafish by germ-line replacement. *Proc. Natl Acad. Sci. USA* **99,** 14919–14924 (2002).
15. Heisenberg, C. P. *et al.* Silberblick/Wnt11 mediates convergent extension movements during zebrafish gastrulation. *Nature* **405,** 76–81 (2000).
16. Rauch, G. J. *et al.* Wnt5 is required for tail formation in the zebrafish embryo. *Cold Spring Harb. Symp. Quant. Biol.* **62,** 227–234 (1997).
17. Matsui, T. *et al.* Noncanonical Wnt signaling regulates midline convergence of organ primordia during zebrafish development. *Genes Dev.* **19,** 164–175 (2005).
18. Wallingford, J. B. & Harland, R. M. *Xenopus* Dishevelled signaling regulates both neural and mesodermal convergent extension: parallel forces elongating the body axis. *Development* **128,** 2581–2592 (2001).
19. Thisse, C. & Thisse, B. Antivin, a novel and divergent member of the TGFβ superfamily, negatively regulates mesoderm induction. *Development* **126,** 229–240 (1999).
20. Meno, C. *et al.* Mouse Lefty2 and zebrafish antivin are feedback inhibitors of nodal signaling during vertebrate gastrulation. *Mol. Cell* **4,** 287–298 (1999).
21. Ando, R., Hama, H., Yamamoto-Hino, M., Mizuno, H. & Miyawaki, A. An optical marker based on the UV-induced green-to-red photoconversion of a fluorescent protein. *Proc. Natl Acad. Sci. USA* **99,** 12651–12656 (2002).
22. Strutt, D. I. The asymmetric subcellular localisation of components of the planar polarity pathway. *Semin. Cell Dev. Biol.* **13,** 225–231 (2002).
23. Jiang, D., Munro, E. M. & Smith, W. C. Ascidian prickle regulates both mediolateral and anterior–posterior cell polarity of notochord cells. *Curr. Biol.* **15,** 79–85 (2005).
24. Jenny, A., Darken, R. S., Wilson, P. A. & Mlodzik, M. Prickle and Strabismus form a functional complex to generate a correct axis during planar cell polarity signaling. *EMBO J.* **22,** 4409–4420 (2003).
25. Lyons, D. A. *et al.* erbb3 and erbb2 are essential for Schwann cell migration and myelination in zebrafish. *Curr. Biol.* **15,** 513–524 (2005).
26. Gong, Y., Mo, C. & Fraser, S. E. Planar cell polarity signalling controls cell division orientation during zebrafish gastrulation. *Nature* **430,** 689–693 (2004).
27. Djiane, A., Yogev, S. & Mlodzik, M. The apical determinants aPKC and dPatj regulate Frizzled-dependent planar cell polarity in the *Drosophila* eye. *Cell* **121,** 621–631 (2005).
28. van Straaten, H. W. & Copp, A. J. Curly tail: a 50-year history of the mouse spina bifida model. *Anat. Embryol. (Berl.)* **203,** 225–237 (2001).
29. Gritsman, K. *et al.* The EGF-CFC protein one-eyed pinhead is essential for nodal signaling. *Cell* **97,** 121–132 (1999).
30. Carreira-Barbosa, F. *et al.* Prickle 1 regulates cell movements during gastrulation and neuronal migration in zebrafish. *Development* **130,** 4037–4046 (2003).

Supplementary Information is linked to the online version of the paper at www.nature.com/nature.

Acknowledgements We thank W. Talbot and D. Lyons for sharing their protocol for pharmacological inhibition of cell division, A. Chitnis for useful discussion, and L. Solnica-Krezel, W. Talbot, J. Wallingford, A. Giraldez, D. Prober and J. Rihel for comments on the manuscript. This work was supported by grants from the NIH to A.F.S. and M.M. A.F.S. was a Scholar of the McKnight Foundation for Neuroscience, an Irma T. Hirschl Trust Career Scientist and an Established Investigator of the American Heart Association. B.C. was supported by a long-term fellowship from the Human Frontier Science Program.

Author Information Reprints and permissions information is available at npg.nature.com/reprintsandpermissions. The authors declare no competing financial interests. Correspondence and requests for materials should be addressed to B.C. (ciruna@sickkids.ca) or A.F.S. (schier@fas.harvard.edu).